Aerothermochemistry Testing of a Ceramic Matrix Composite TPS for a Lifting Reentry Vehicle

Francesco Panerai, Olivier Chazot**, Bernd Helber***, Isil Sakraker****,*
Thierry Pichon[+], Renaud Barreteau[++]
**PhD Candidate at von Karman Institute for Fluid Dynamics*
francesco.panerai@vki.ac.be
*** Associate Professor at von Karman Institute for Fluid Dynamics*
olivier.chazot@vki.ac.be
****PhD Candidate at von Karman Institute for Fluid Dynamics*
bernd.helber@vki.ac.be
*****PhD Candidate at von Karman Institute for Fluid Dynamics*
isil.sakraker@vki.ac.be
[+]Program Manager IXV, Snecma Propulsion Solide
thierry.pichon@snecma.fr,
[++]Project Manager IXV, Snecma Propulsion Solide
renaud.barreteau@snecma.fr

Abstract

This paper summarizes the results of an experimental campaign devoted to characterization of the Intermediate eXperimental Vehicle Thermal Protection System. Ceramic materials selected for the assembly of the IXV windward-side were tested in the Plasmatron facility at the von Karman Institute for Fluid Dynamics, with the objective of reproducing the aerothermochemical environment experienced by the vehicle during the atmospheric reentry. Emissivity and catalycity properties were determined for wall temperatures from 1200 to 2000 K and pressures between 1300 and 5000 Pa. The testing methodology included experimental data coming from intrusive and optical infrared measurements as well as numerical data processing devoted to the rebuilding of enthalpy conditions and boundary layer chemical composition. Variation of catalytic properties with flow conditions and surface temperature were discussed. Emissivity changes with surface temperature and oxidation status were also compared with data extracted from room temperature reflectivity measurements. Further characterization of the material was performed using new developed probes for off-stagnation testing, with the aim of better simulating in the Plasmatron ground facility the vehicle windward side region.

1. Introduction

Space vehicles reentering a planetary atmosphere require specific Thermal Protection Systems (TPS) to withstand aerothermodynamic loads along their trajectory. When the spacecraft approaches a relatively dense atmosphere, a strong bow shock takes place ahead of the nose. Across the shock a large amount of kinetic energy is converted into thermal energy which leads to high temperatures of the gas mixture where dissociation and ionization phenomena take place. The result is a chemically reacting flow impinging on the vehicle walls.

Dissociated species reaching the heat shield eventually recombine in exothermic reactions promoted by the catalytic nature of the surface. Catalysis phenomena strongly affect the design of a reusable TPS. A fully catalytic wall can double the heat flux with respect to a non catalytic wall. Furthermore, in the real TPS scenario catalysis processes go together with other mechanisms that determine the global behavior of the heat shield. Radiative effects, that is the cooling process due to high temperature and emissivity ("), and oxidation/nitridation phenomena, that is the interaction between the TPS and oxygen/nitrogen species, drive together with catalycity ( ) the global heat flux balance at the wall.

The catalytic nature of a TPS describes the behavior of the material to act as a catalyst for recombination reactions of the atomic species in the surrounding gas mixture. Since highly exothermic, surface reactions release a considerable

quota of the heat flux to the wall. As a rule of thumb one can state that the heat flux can be halved by choosing an ideal non catalytic material. Radiative phenomena are also important, as they drive the only cooling process for passive reusable TPS. The radiative heat flux depends on the TPM emissivity, i.e. the ratio of the actual radiated energy per unit time over the theoretical maximum limit.

Catalycity and radiative phenomena act together with surface erosion processes, like oxidation and nitridation, which are driven by temperature and species partial pressure at the surface. The combination of all the describes phenomomena on a reausable TPS are referred as gas/surface interactions (GSI). Relevant effort has been spent since the early Space Shuttle flights towards the characterization of GSI processes. Outstanding works can be found in literature on catalytic, radiative and oxidation properties of CMC, investigated in different types of ground facilities (arc-jets, ICP wind tunnels, diffusion reactors, etc.). Nevertheless the varaition of such porperties is, in most of the cases, referrend to surface temperature conditions only, while a detailes a detailes description of the chemical environment (pressure, concentrations, etc.) is poorly addressed. Additionally, the behavior of GSI phenomena with different flight conditions and, more generally, extrapolation to flight is far to be thoroughly undestood.

In this paper we analyze the results of an experimental campaign on CMC specimens carried out at the von Karman Institute for Fluid Dynamics (VKI), aimed to characterize the TPS of the Intermediate eXperimental Vehicle (IXV), under development at the European Space Agency. A C/SiC material is chosen for the nose and the windward side TPS, which are the most critical areas, during the IXV lifting reentry.

Catalycity and emissivity properties of material under investigation, introduced in a recent publication, are re-called here. Additional description of specific testing condition for the windward side of the lifting body vehicle are also presenting with the first results obtained in this configuration.

2. Experimental Setup

The experimental measurements are conducted in the VKI Plasmatron. This is a high enthalpy wind tunnel in which plasma is generated by electromagnetic induction and blown in the form of a subsonic jet inside a test chamber at sub-atmospheric pressure (between 5 and 200 mbar). The facility, which is the most powerful induction-coupled plasma (ICP) wind tunnel in the world, uses a high frequency, high power, high voltage (400 kHz, 1.2 MW, 2 kV) solid state (MOS technology) generator, feeding the single-turn inductor of the 160 mm diameter plasma torch. The torch is mounted on a 1.4 m diameter, 2.5 m long, water-cooled test chamber, fitted with different portholes that allow unrestricted optical access to the test section. A 5 cm diameter copper water cooled probe is used for the calibration of plasma flow conditions. A copper calorimeter placed in the center of the front face is able to measure the cold wall (350 K) heat flux at the stagnation point. This is determined by the mass flow (controlled by a calibrated rotameter) and the cooling water temperature difference between the inlet and outlet sections, measured by two type E thermocouples also calibrated prior to the test, by means of a uniform temperature oil bath and a reference mercury thermometer. In order to have correct measurements, the sidewalls of the calorimeter have to be adiabatic, therefore a Teflon insulator is installed between the calorimeter and the wall of the probe for this purpose. Both the probe and calorimeter have polished copper surfaces which are high catalytic to nitrogen and oxygen atom surface recombination.

The heat flux is given by:

$$q_{cw} = \frac{\dot{m} \cdot C_p \cdot (T_{out} - T_{in})}{A}$$

The error on this measurements is estimated to be ±10%. A water cooled Pitot probe is used to measure dynamic pressure. The pressure line is connected to a pressure transducer, which is calibrated prior to the test. Such measurements are 7% accurate. The sample holder, which has the same geometry of the heat flux probe, is composed of two coaxial tubes in which water circulates for cooling. At the extremity, a support for the sample made of SiC is attached to the holder body by three metallic pins. A thick insulation layer of Procelit R 180 is placed as back support for the sample in order to limit the heat flux dispersion by conduction. The test specimens are 3 cm diameter disk samples (standard Europeanmodel)made of C/SiC, produced at Snecma Propulsion Solide (Le Haillan, France) [6, 7]. Two Raytek Marathon Series (Raytek Corp., Santa Cruz, CA) pyrometers record the front surface temperature of the sample. They are chosen alternatively according to the target and the measurement range (700-1800 ◦C for the MR1SB and 1000-3000 ◦C for the MR1SC). As two- color pyrometers they measure over two overlapping narrow wavebands around 1 µm, providing an output value independent on emissivity. They are pointed and focused to the stagnation point of the sample and look through a quartz window of 1 cm thickness. The pyrometers are calibrated by

means of a blackbody reference source together with the quartz window. The overall uncertainty of pyrometermeasurements is estimated to be 10 ◦C. The pyrometer records the signal at 1 Hz.

An Heitronics KT19 (HEITRONICS Infrarot Messtechnik GmbH, Wiesbaden, Germany) infrared radiometer is located in front of a 1.8 cm thick KRS-5 window and is used for radiance measurements. The radiometer operates in the wavelength range of 0.6 to 39 µm and provides as output the integrated thermal radiation over this spectrum, within a temperature range of 0 to 3000 ◦C, at 1 Hz acquisition rate. Like the pyrometers, the radiometer is calibrated using a blackbody radiation source together with the corresponding window. The probes are mounted inside the Plasmatron test chamber at 0.445 m distance from the nozzle exit. The placement ensures that the axis of the probe and the axis of the nozzle coincide.

3. Testing Methodology

The reproduction of flight conditions in the Plasmatron facility relies on the Local Heat Transfer Simulation (LHTS) concept. The methodology, developed at the Institute for Problems in Mechanics of Moscow (IPM) [8] and adopted at the VKI [9], is a derivation of the theory of stagnation-point heat transfer in chemically reacting flows developed by Fay and Riddell [10] and Goulard [11] in the late fifties. It has been shown that a complete duplication of the real hypersonic flight can be achieved in a ground subsonic facility if the flight total enthalpy Hf, the total pressure Pf and the velocity gradient duf/dx are locally matched on the test article.

3.1. Catalycity determination

Based on LHTS, the process of catalycity prediction by Plasmatron testing in stagnation point configuration combines experimental measurements and CFD data. Simulations of the subsonic Plasmatron flowfield, under Local Thermochemical Equilibrium (LTE) and axisymmetric flow assumptions, are performed by means of the VKI ICP Code [12]. Further, the VKI Boundary Layer Code [13] solves the equations of the reacting boundary layer over a catalytic surface, under the assumption of Chemical Non-EQuilibrium (CNEQ) and axisymmetric flow, providing computations of the stagnation point heat flux as a function of wall temperature Tw, catalycity γ and boundary layer properties. The thermodynamic and transport properties of air are determined by means of the PEGASE library [14]. The VKI Rebuilding Code iterates on the boundary layer outer edge temperature Te, until experimental and numerical heat flux are matched, so that the Boundary Layer Code provides outer edge enthalpy he and velocity ve as outputs. Catalycity values can be finally identified by intersecting the experimental conditions $Q^{exp}w$ and $T^{exp}w$ on an heat flux abacus qw = qw (Tw, γ), built by the Boundary Layer Code (two examples are given in Section 4, Figure 11). It is remarked that the hot wall experimental heat flux is calculated by radiative equilibrium wall assumption. The contribution coming from the conduction term is neglected (Qcond = 0), so that the heat flux is slightly underestimated. The error induced by this assumption is negligible with respect to the uncertainty in the cold wall heat flux.

3.2. Emissivity measurements

Directional emissivity values can be determined in-situ from Plasmatron infrared measurements. By definition the total emissivity is the ratio between the object radiance L and the blackbody radiance L0 at the same conditions of temperature and wavelength. The blackbody radiance at a given temperature is know if the temperature is known and can therefore be calculated by means of 2-color pyrometer measurements (which are emissivity independent). The infrared radiance of the sample is instead measured by the radiometer in the 0.6-39 µm infrared range. Therefore the total emissivity at a certain temperature is given by:

$$\varepsilon = \frac{L}{L^0}$$

Emissivities can be also estimated by spectral reflectivity room-temperature measurements on virgin samples prior to plasma exposure. A Cary-500 VARIAN spectrophotometer working from the ultraviolet to the near infrared waveband (0.25 to 2.5 µm) is used together with Bruker IFS66v Fourier Transform Infrared Spectrometer operating

from near infrared to medium infrared (2.5 to 40 µm). The measurements are performed at the ESA ESTEC center (Noordwijk, The Netherlands) facilities. Correcting the measured reflectivity by Kirchhoff's law and weighting by the Planck's radiation distribution function E(λ, T) the total emissivity as a function of the wall temperature reads:

$$\varepsilon(T) = \frac{\int_{0.25\mu m}^{40\mu m} (1 - r(\lambda)) E(\lambda, T)\, d\lambda}{\int_{0.25\mu m}^{40\mu m} E(\lambda, T)\, d\lambda}$$

4. TPS testing

4.1. Stagnation point operating conditions

The Plasmatron tests are performed under standard air plasma (80% N2 and 20% O2) at a mass flow of 16 g/s. Table 1 describes the test conditions: surface temperature and chamber static pressure are chosen as target conditions according to the IXV flight trajectory.

Table 1: Test conditions matrix

Test	Tw	PW	P_S	q_{cw}	P_d
	[K]	[kW]	[Pa]	[kW/m^2]	[Pa]
1	1400	99	1320	360	83
2	1400	104	1980	385	60
3	1400	133	3020	410	60
4	1400	124	4020	375	35
5	1400	130	5000	390	27
6	1600	152	1320	745	160
7	1600	158	2010	735	115
8	1600	158	3000	810	75
9	1600	178	4000	745	75
10	1600	189	4960	700	55
11	1800	235	1340	1150	235
12	1800	242	1980	1250	175
13	1800	253	2990	1280	130
14	1800	230	4000	1300	80
15	1800	236	5000	1215	80
16	2000	287	1330	1510	305
17	2000	292	1970	1490	220
18	2000	312	2990	1570	170
18a	2000	308	2990	1540	165
19	2000	331	4010	1655	150
20	2000	300	5000	1775	105
21	1200	84	1340	195	75
22	1200	93	2000	185	65
23	1200	95	3020	180	45
24	1200	99	3960	175	32
25	1200	105	4970	160	25

The reference temperature is measured at the center of the sample, on the surface exposed to the plasma flow, by the 2-color pyrometer. The generator power is adjusted in order to have the desired temperature target and pressure

values specified are maintained constant thanks to air by-pass and vacuum pumps regulation. At steady state conditions, the samples are exposed to the plasma stream for a total of 3 min test time. Flow conditions are calibrated right after the TPS exposure to plasma by means of the calorimetric and pressure probes which are maintained into the plasma stream until steady state conditions are well established. Figures 1 and 2 show an example of temperature and reference heat flux measurements for test 17.

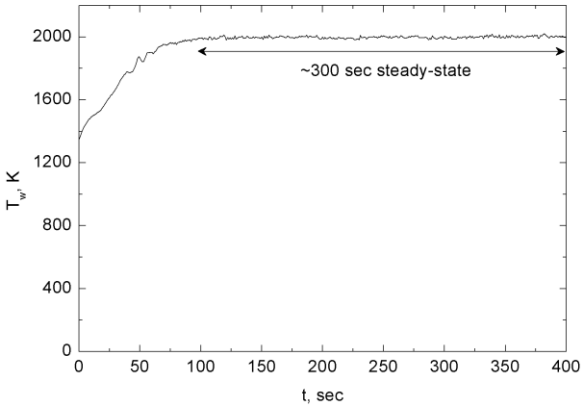

Figure 1: Surface temperature for test 17

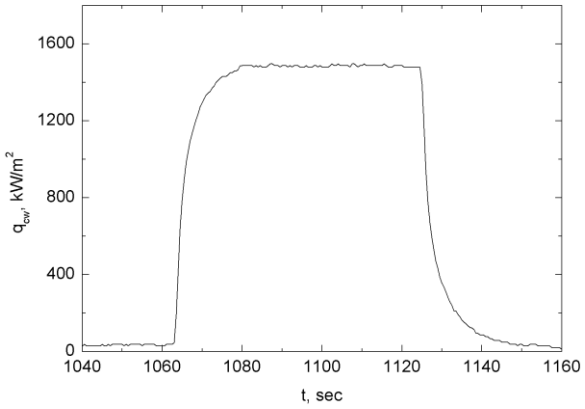

Figure 2: Cold wall heat flux measurements for test 17

4.2. Enthalpy rebuilding and extrapolation to flight

The boundary layer environment for each test case was numerically rebuilt following the methodology explained in Section 3, throughwhich enthalpy, temperature and ve- locity at the boundary layer outer edge can be determined. Enthalpy versus pressure conditions are compared with the IXV flight trajectory in Figure 3. The flight data are computed as [9]:

$$H_{\text{tot}}^{\text{f}} = h_{\infty}^{\text{f}} + \frac{1}{2} V_{\infty}^{2\text{f}}$$

$$p_{\text{tot}}^{\text{f}} = p_{\infty}^{\text{f}} + \rho_{\infty}^{\text{f}} V_{\infty}^{2\text{f}}$$

considering that at hypersonic speeds the first terms of the two formulas are negligible. One can see that the test conditions cover the relevant part of the reentry. Particularly the cases at 1600 K and 1800 K offer the best reproducibility of the real case.

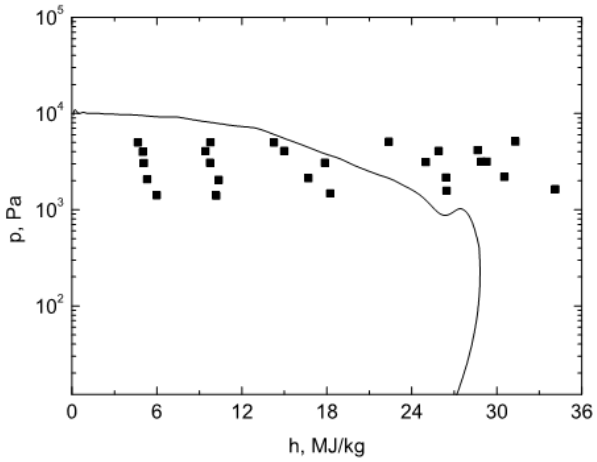

Figure 3: Comparison between the IXV flight trajectory and the rebuilt test conditions.

4.3. TPS emissivity database

Emissivity values are calculated according to Equation 2. These are shown in Figure 4 which highlights the high radiative nature of the material, given by an ε that is overall higher that 0.7 at high temperatures. One can observe an improvement of radiative properties of the TPS as the temperature raises from 1200 to 1600 K. For higher temperatures this trend is inverted and the emissivity decreases to lower values as a consequence of surface optical properties degradation. Minor differences can be instead noticed with pressure conditions. Different statuses of the test environment in terms of pressure and temperature lead to different oxidations of the samples surface, which correspond to different optical properties, i.e. different emissivity. The diverse surface oxidation can be clearly noticed observing the samples surface in Figure 7. Typically at low temperatures the material undergoes passive oxidation, that is an SiO2 layer is formed over the surface [15]. The thickness of such layer increases from the order of Ångström (brownish color, sample 6a) to few microns (yellowish color, sample 6c), which corresponds to an improvement of emissivity from ~ 0.75 to ~ 0.85. Higher temperatures lead to different oxidation mechanisms that result in a dark gray color at 1800 K (sample 6d) and then a light gray one (sample 6e). The variation of the processes described depends also on pressure, even though such variations are less evident and regular.

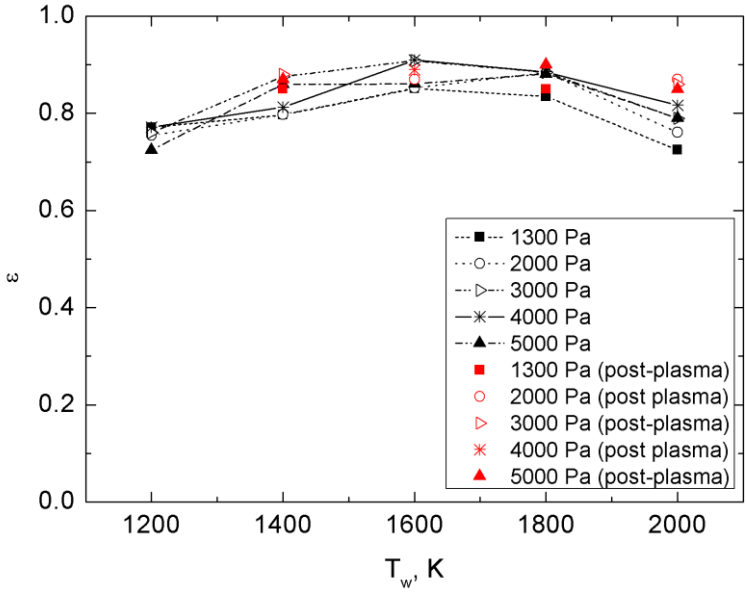

Figure 4: In-situ emissivity measurements and comparison with post-plasma room temperature measurements.

Total emissivity values are extracted for room temperature reflectivity measurements after plasma exposure according to Equation 3. The extrapolated values at the plasma test temperature are compared with in-situ measurements (red dots in Figure 4). The agreement between the two techniques is excellent.

A temperature-dependent model of emissivity is built fitting the experimental data. The data available for flight condition cover the range 1200-2000 K. Additionally, room temperature measurements performed on virgin samples provide emissivity values at 300 K and 400 K. A 4th order polynomial curve is chosen to fit both Plasmatron data at reentry conditions and room temperature values. The result is shown in Figure 5 together with the correspondent error bands. The fitting law predicts that the emissivity does not vary in the range 400-1100 K (where no experimental data at temperature are available). This can be considered reasonable, as only negligible surface changes due to oxidation processes are expected for such low temperatures. 2100 K is assumed as the upper applicability limit as for higher temperatures strong active oxidation phenomena become the leading processes, implying radical surface modification that cannot be handled by the present model. If the fitting law is compared with the emissivity extrapolation obtained from room temperature measurements, as shown in Figure 6, one can notice that the model underestimates emissivity values in the 400-1100 K range and above 2000 K, which is conservative for design calculations.

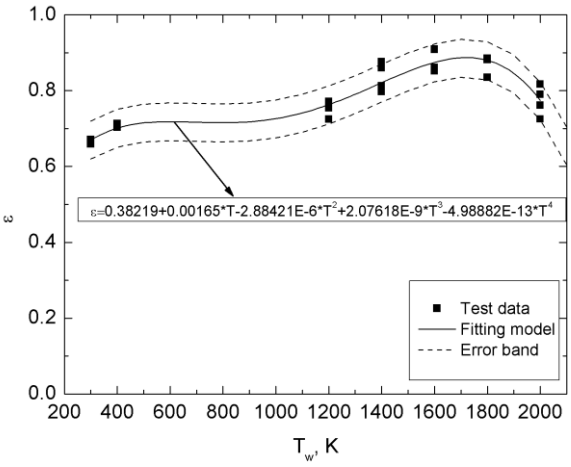

Figure 5: Emissivity model for the IXV thermal protection system.

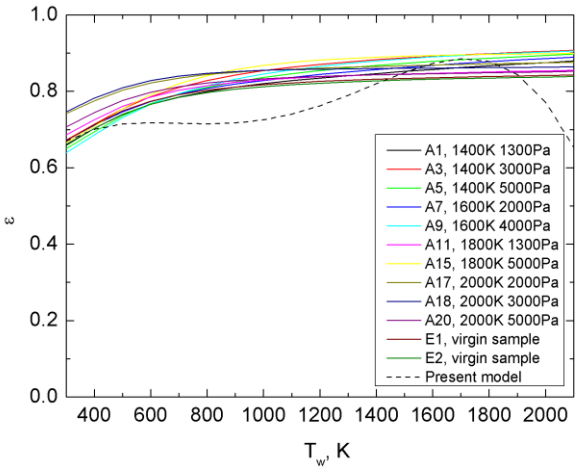

Figure 6: Comparison of the model with room temperature measurements.

(a) 1200 K (b) 1400 K (c) 1600 K (d) 1800 K (e) 2000 K

Figure 7: Change of surface appearance for different test conditions.

4.4. TPS Catalycity database

Catalycity values calculated by data processing of Plasmatron measurements are illustrated in Figure 8 where γ is plotted as a function of wall temperature for different pressures imposed. One can notice that catalycity decreases with temperature from 1200 K to 1400 K and increases for temperatures higher that 1400 K up to 2000 K. Lower values of pressure yield higher catalycity andnvice versa. The results allow to compute a reduction of 50-60% with respect to the full catalytic assumption at the same temperature, which higlights the low catalycity of the material.

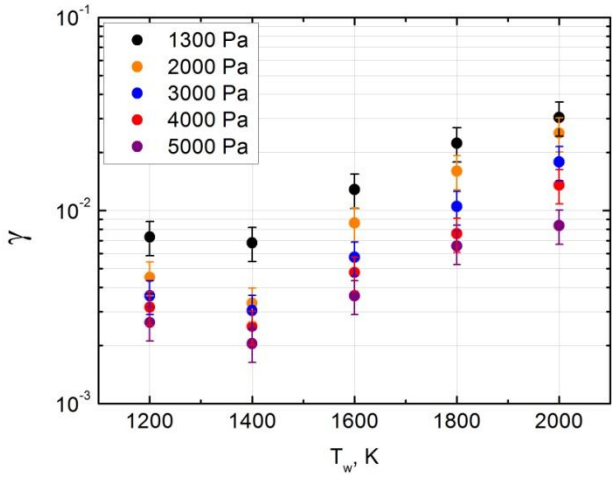

Figure 8: Determined catalycity values for the different plasma conditions.

The results summarized for the effective recombination coefficients for the CMC TPS samples are obtained from experimental measurements and a data processing taking into account a chemistry model for the chemical non-equilibrium in the boundary layer and a model for the wall recombination assuming $\gamma_O = \gamma_N = 1$. The error bars reported are indicative coming from the measurement accuracy, a more precise definition of such uncertainty need a dedicated approach as it has been mentioned in [16]. The results exhibit some trends that could be interpreted in the frame of the models used considering classical stagnation point heat-transfer expression for dissociated gases. Nevertheless it has to be noted that many phenomena happen together, even considering the macroscopic quantities, so the remarks given are illustrative and cannot stand for a final explanations or demonstrations. A physical interpretation of the catalycity behavior with respect to the pressure and temperature variation has been exposed in a previous publication [16].

4.5. Off-Stagnation point Testing

A new testing configuration, addressing off-stagnation point situation, has been developed in the VKI Plasmatron. The associated testing methodology has been assessed by numerical computation and cold wall heat-flux measurements [17]. Specific probe and sample holder have been designed and tested for these experiments. They allow to address heat-flux duplication from reaction boundary layers in specific flight conditions [18].

Thus a second test campaign involved the testing of CMC samples in off-stagnation point configuration. Rectangular TPS samples of 152x30 mm were inserted into the flat plate sample holder. The testing conditions have been characterized with the stagnation point heat-flux probe to determine the free stream enthalpy. A radiometer, a 2-colors pyrometer and an IR camera were set up on the lateral side of the test section to allow surface measurements (fig. 9).

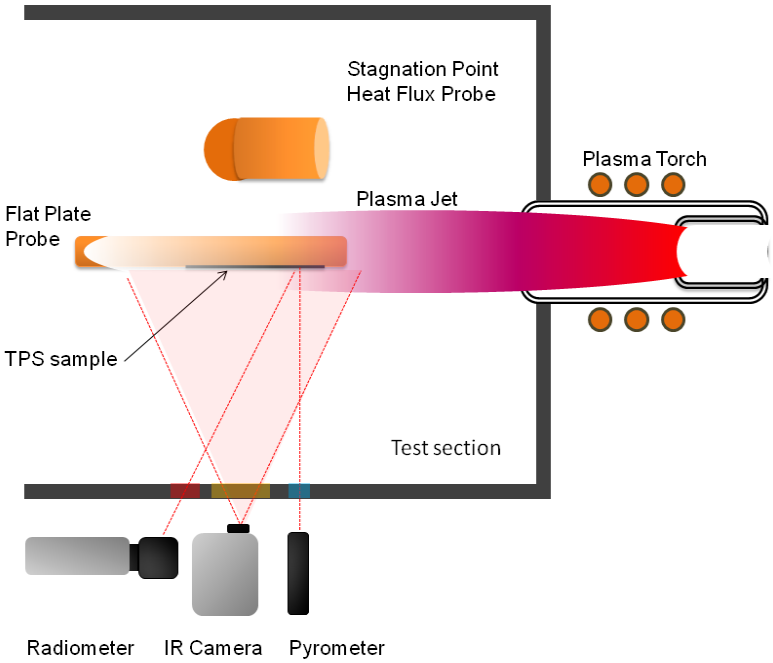

Figure 9: Schematic representation of the test setup

In the frame of the design activities for the CATE in-flight experiments three type of samples have been tested: a low catalytic CMC sample, which represents the baseline TPS material for IXV, from SPS, a high catalytic sample realized with a Mullite coating ($3Al_2O_32SiO_2$) applied by thermal-spray process over the CMC TPS, and a combined sample only partially coated to exhibit a catalytic transition for the simulation of the CATE experiment. The testing conditions were set to a free stream enthalpy of 20 MJ/kg under 1500 Pa. Typical results are shown in figure 10. Emissivity properties of the Mullite coating and the baseline CMC were found to be very close [19]. This result helps to have a direct interpretation of the temperature profiles recorded from the IR camera for the three samples tested.

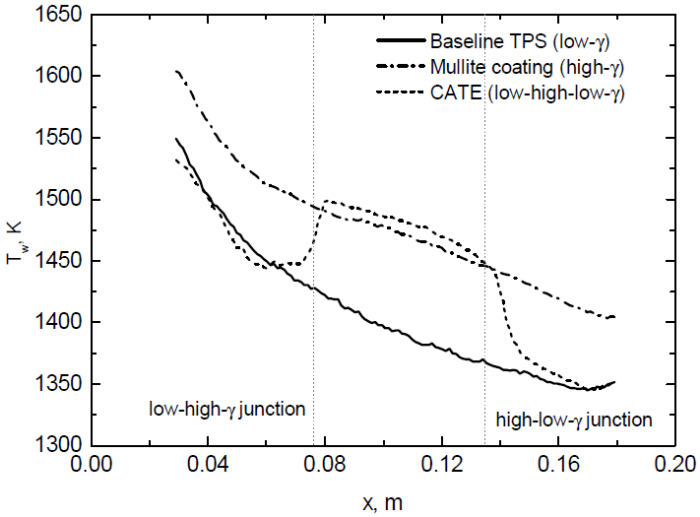

Figure 12: Temperature profile along the TPS samples tested: CMC, Full coating, Partial coating

A temperature jump is clearly visible at the location of the catalytic transition and could be identified as a effect of the GSI phenomena. Further testing will need to be carried out for a better determination of the phenomena along the vehicle trajectory since GSI depends not only on the surface properties but also on the flow conditions. In this context the off-stagnation point testing offer a suitable framework to support the flight experiments.

5. Conclusion

A summary have been presented of the experimental activities carried out at VKI Plasmatron facility in the framework of the IXV mission, for the characterization of the ceramic Thermal Protection Material of the vehicle nose and windward side. The samples have been tested for representative flight conditions. The material has showed high emissivity and low catalytic nature which are ideal properties for thermal protection. The development of a new methodology for off-stagnation point testing in a plasma wind tunnel was also presented. The first results appear very promising and open nice opportunities for new testing and qualification.

6. Acknowledgements

The experimental campaign and the dataprocessing were supported by Snecma Propulsion Solide (Le Haillan, France) and Dassault Aviation (Saint-Cloud, Paris) contracts. Snecma Propulsion Solide provided the specimens used during the test campaign. The authors are grateful to Mr. Pascal Collin for his unique dedication to the operation of the Plasmatron facility. Emissivity measurements have been performed at the Materials Space Evaluation & Radiation Effects Section at European Space Agency, ESTEC (Noordwijk, The Netherlands).

References

[1] M. J. H. Balat, M. Czerniak, and J. M. Badie. Ceramics Catalysis Evaluation at High Temperature Using Thermal and Chemical Approaches. Journal of Spacecraft and Rockets, 36(2):273–279, March-April 1999.

[2] D. A. Stewart. Determination of Surface Catalytic Efficiency for Thermal ProtectionMaterials – Room Temperature to Their Upper Use Limit. In 31st AIAA Thermophysics Conference, AIAA 96-1863, New Orleans, LA,USA, June 1996.

[3] A. F. Kolesnikov, I. S. Pershin, S. A. Vasil'evsky, and M. I. Yakushin. Study of Quarz Surface Catalicity in Dissociated Carbon Dioxide Subsonic Flows. Journal of Spacecraft and Rockets, 37(5):573–579, 2000.

[4] G. Tumino. IXV: the Intermadiate eXperimental Vehicle. ESA Bulletin 128, November 2006.

[5] H. W. Krassilchikoff, O. Chazot, and J. Thoemel. Procedure for the Determination of Cold Copper Recombination Efficiency. In 2nd European Conference for Aero-Space Sciences, Bruxelles, Belgium, July 2007.

[6] T. Pichon, P. Soyris, A. Foucault, J. M Parenteau, Y. Prel, and S. Guedron. C/SiC Based Rigid External Thermal Protection System for Future Reusable Launch Vehicles: Generic Shingle, Pre-X/FLPP Anticipated Development Test Studies. In 5th European Workshop Thermal Protection Systems and Hot Structures, 2005.

[7] T. Pichon, R. Barreteau, P. Soyris, A. Foucault, J.M Parenteau, Y. Prel, and S. Guedron. CMC thermal protection system for future reusable launch vehicles: Generic shingle technological maturation and tests. Acta Astronautica, 65(1-2):165–176, 2009.

[8] A. F. Kolesnikov. Conditions of Simulation of Stagnation Point Heat Transfer from a High-enthalpy Flow. Fluid Dynamics, 28(1):131–137, January 1993.

[9] P. F. Barbante and O. Chazot. Flight Extrapolation of Plasma Wind Tunnel Stagnation Region Flowfield. Journal of Thermophysics and Heat Transfer, 20(3):493–499, July-September 2006.

[10] J. A. Fay and F. R. Riddell. Theory of Stagnation Point Heat Transfer in Dissociated Air. Journal of Aeronautical Science, 25(2):73–85, February 1958.

[11] R. Goulard. On Catalytic Recombination Rates in Hypersonic Stagnation Heat Transfer. Jet Propulsion, 28(11):737–745, November 1958.

[12] G. Degrez, D. P. Vanden Abeele, P. F. Barbante, and B. Bottin. Numerical Simulation of Inductively Coupled Plasma Flows under Chemical Non-equilibrium. International Journal of Numerical Methods for Heat & Fluid Flow, 14(4):538–558, 2004.

[13] P. F. Barbante, G. Degrez, and G. S. R. Sarma. Computation of Nonequilibrium High Temperature Axisymmetric Boundary-Layer Flows. Journal of Thermophysics and Heat Transfer, 16(4):490–497, 2002.

[14] B. Bottin, D. P. Vanden Abeele, M. Carbonaro, G. Degrez, and G. S. R. Sarma. Thermodynamic and Transport Properties for Inductively Plasma Modeling. Journal of Thermophysics and Heat Transfer, 13(3):343–350, 1999.

[15] M. Balat, G. Flamant, G. Male, and G. Pichelin. Active to passive transition in the oxidation of silicon carbide at high temperature and low pressure in molecular and atomic oxigen. Journal of Materials Science, 27:697–703, 1992.

[16] Panerai F., B. Helber, I. Sakraker, O. Chazot, T. Pichon, R. Barreteau, J. P. Tribot, JJ Vallée, V. Mareschi, D. Ferrarella, G. Rufolo, and S. Mancuso; Characterization of the IXV thermal protection system in high enthalpy plasma flow, ESA ATD Symposium, Bruges, May 9-12, 2011.

[17] Chazot O., F. Panerai, V. Van Der Haegen; Aerothermochemistry Testing for lifting body re-entry vehicles, ESA ATD Symposium, Bruges, May 9-12, 2011.

[18]. Chazot O and Panerai, F., Off-Stagnation Point Testing and Methodology in Plasma wind tunnel, 17th AIAA International Space Planes and Hypersonic Systems and Technologies Conference, San Francisco, CA, 11 - 14 Apr 2011.

[19] Panerai, F. and Chazot O., Plasma wind tunnel testing as support to the design of Gas-Surface Interaction in-flight experiments, 17th AIAA International Space Planes and Hypersonic Systems and Technologies Conference, San Francisco, CA, 11 - 14 Apr 2011.